J. Fluid Mech. (1982), *vol.* 121, *pp.* 283–299
Printed in Great Britain

An extended channel model for the prediction of motion in elongated homogeneous lakes. Part 3. Free oscillations in natural basins

By GABRIEL RAGGIO AND KOLUMBAN HUTTER

Laboratory of Hydraulics, Hydrology and Glaciology, The Federal Institute of Technology, Zurich, Switzerland

(Received 30 December 1980 and in revised form 28 September 1981)

The extended channel model derived and analysed in two previous articles is further developed by investigating free oscillations and forced motion in natural enclosed basins. Firstly, a zeroth-order model is analysed. In this model, field variables are expressed as a product of a single known cross-sectional shape function and an unknown function of time and the co-ordinate along the lake axis. Conditions are discussed under which this zeroth-order model is meaningful, and it is shown that under normal circumstances Coriolis effects must be ignored. Subsequently the general Nth-order channel model is applied to the Lake of Lugano. It is shown that eigenfrequencies and amphidromic systems are well predicted in such channel-like lakes. The paper ends with a discussion on the selection of shape functions and with further applications and limitations of the channel model.

1. Introductory remarks

This paper continues an analysis of the gravitational oscillations of homogeneous water bodies in basins on the rotating Earth (see Raggio & Hutter 1982*a* for general theory, 1982*b* for first applications, referred to henceforth as I and II respectively). Here, this analysis is continued by presenting the results of a numerical study of gravitational oscillations. Such analyses are usually performed by recourse to finite-difference (Rao 1966, 1973, 1977; Rao & Schwab 1976; Schwab 1978) or finite-element (Hamblin 1972, 1976) formulations. We proposed instead a procedure by which the spatially two-dimensional (or in more general situations, the three-dimensional) boundary-value problem was transformed to a hierarchy of boundary-value problems in one spatial dimension. The emerging initial boundary-value problem is then solved by whichever method is suitable for partial differential equations in one space and one time variable. In the subsequent treatment we study some numerical properties of these channel equations.

The transformation of the boundary-value problem to a hierarchy of different boundary-value problems in a lower-dimensional space is given in I. In the literature such spatially reduced models are not in general regarded as numerical procedures approximating a physical problem of higher dimension. Here this viewpoint is adopted, and it will be demonstrated that the channel equations constitute a reasonable model for the description of free oscillations in natural curved elongated lakes, and that a first-order model generally suffices for a reasonable prediction of the motion. Emphasis

will be on the physical appropriateness rather than the numerical properties of the governing equations. These will be investigated more thoroughly in another article (see Raggio 1982). As test basin for our presentation the Lake of Lugano will serve.

This article is the continuation of two previous papers. Equations of these latter articles used herein will be listed with prefix I or II: hence (II2.26) is equation (2.26) of II, etc.

2. Model equations – remarks on a zeroth-order model

Governing equations are (I4.6), (I4.8), (I4.9) and (I4.11), which on ignoring non-linear convective terms assume the form

$$\rho_0\left\{\mathbf{C}^{(1)}\frac{\partial \mathbf{v}_s}{\partial t}-f\mathbf{C}^{(1)}\mathbf{v}_n+g\hat{\mathbf{C}}^{(0)}\frac{\partial \xi}{\partial s}\right\}+\mathbf{R}^{(1)}\mathbf{v}_s+\mathbf{p}_s^{*(0)}-\mathbf{w}_s^{*(1)}=0, \tag{2.1a}$$

$$\rho_0\left\{\mathbf{C}^{(1)}\frac{\partial \mathbf{v}_n}{\partial t}+f\mathbf{C}^{(1)}\mathbf{v}_s+g\hat{\mathbf{C}}_{\phi_n}^{(1)}\xi\right\}+\mathbf{R}^{(1)}\mathbf{v}_n+\mathbf{p}_n^{*(1)}-\mathbf{w}_n^{*(1)}=0, \tag{2.1b}$$

$$\hat{\mathbf{Z}}^{(1)}\frac{\partial \xi}{\partial t}+\frac{\partial}{\partial s}(\mathbf{C}^{(0)}\mathbf{v}_s)-\mathbf{C}_{\phi_n}^{(1)}\mathbf{v}_n-\mathbf{C}_{\phi_n}^{(1)}\mathbf{v}_z=0, \tag{2.1c}$$

$$\mathbf{H}_s^{(0)}\mathbf{v}_s+\mathbf{H}_n^{(1)}\mathbf{v}_n-\mathbf{H}^{(1)}\mathbf{v}_z=0. \tag{2.1d}$$

Here $\mathbf{v}_s$, $\mathbf{v}_n$, $\mathbf{v}_z$ are unknown vector quantities representative of the velocity components in the longitudinal, transverse and vertical directions of the curvilinear co-ordinate system (s, n, z), and ξ characterizes the surface elevation. The coefficient matrices are known functions of position s and are defined in appendix A of I, and vector quantities carrying an asterisk are those due to atmospheric pressure and wind forces, also defined in appendix A of I. The physical fields v_s etc. are related to the above vector quantities $\mathbf{v}_s$ etc. by the shape-function expansions $v_s = \boldsymbol{\phi}.\mathbf{v}_s$ etc. and the dimension of $\boldsymbol{\phi}$ or $\mathbf{v}_s$ defines the order of the model. In a zeroth-order model all quantities reduce to scalars. The emerging model is still complicated in this case, but it seems justifiable to ignore the transverse momentum equation and the bottom boundary condition (2.1d), and in the surface continuity equation (2.1c) to omit the third and fourth terms in comparison with the first two terms. The two remaining equations are then the longitudinal momentum equation and the continuity equation involving $\mathbf{v}_s$, ξ and $\mathbf{v}_n$, but the last variable only enters together with the Coriolis parameter and must be ignored. The resulting equations are then (we now drop bold-faced notation)

$$C^{(1)}\frac{\partial v_s}{\partial t}+C^{(0)}g\frac{\partial \xi}{\partial s}+\frac{R^{(1)}}{\rho_0}v_s=\frac{w_s^{*(1)}}{\rho_0}-gC^{(0)}\frac{\partial \xi^*}{\partial s}, \tag{2.2a}$$

$$Z^{(1)}\frac{\partial \xi}{\partial t}+\frac{\partial}{\partial s}(C^{(0)}v_s)=0, \tag{2.2b}$$

in which

$$p_s^{*(0)}=\iint_Q \frac{\partial p_{at}^*}{\partial s}\,dn\,dz=\rho_0 g C^{(0)}\frac{\partial \xi^*}{\partial s}, \tag{2.3a}$$

$$C^{(j)}=\iint_Q J^j\phi^2\,dn\,dz\quad (j=1,2),\quad Z^{(1)}=\int_{B^-}^{B^+}J\phi^2\Big|_{z=0}\,dn \tag{2.3b,c}$$

relate the variable ξ^* with the atmospheric pressure gradient and define the coefficients in terms of cross-sectional integrals. In these $J = 1 - Kn$, where K is the curvature of

the channel axis, Q is the cross-section, and B^+ and B^- are the two shorelines. The coefficients (2.3) depend on the choice of the shape function. This flexibility enhances the applicability of (2.1). For instance, in a rectangular channel one may choose trigonometric functions for ϕ and then deduce the exact solution to the corresponding eigenmode. The coefficients (2.3b, c) are also weighted with the curvature, which eliminates the element of subjectivity when selecting the channel axis, as different choices of channel axes will automatically be accounted for by appropriate changes in the coefficients (2.3).

3. Free oscillations in natural basins

Sufficient proof for the channel model has been given in I and II to regard it as a reasonable description of gravitational modes in narrow elongated lakes. Its governing equations are (2.1a–d), which in that form hold for arbitrary shape-function expansions. They represent the longitudinal and transverse momentum equations, the continuity equation, and the kinematic boundary condition at the bottom. When complemented by initial conditions and appropriate boundary conditions at the channel ends, they will allow determination of surface elevation and velocity distributions either resulting from external forces or as free oscillations. For an Nth-order model (2.1) is a partial differential equation involving the $4N$ unknowns $\mathbf{v}_s$, $\mathbf{v}_n$, $\mathbf{v}_z$, $\boldsymbol{\xi}$; the remaining quantities carrying an asterisk being prescribed external forces (see (II2.6)). For large N computational expenditures may be large, but this disadvantage of the channel model is partly compensated, as a steady-state process and a periodic response (upon a Fourier transformation) will transform the partial differential equations in the variables s and t into a two-point boundary-value problem for an ordinary differential equation, which can be solved by whichever ordinary differential equation integrator is available. Thus writing all variables $\mathbf{v}_s, \ldots, \boldsymbol{\xi}, \mathbf{p}_s^{*(0)}, \ldots, \mathbf{w}_n^{*(1)}$ as $f = f_0 \exp(i\omega t)$ with complex-valued amplitude vector, the following complex-valued set of equations for the amplitudes is obtained (the subscript in f_0 is henceforth deleted):

$$\mathbf{D}.\frac{d\mathbf{y}}{ds} + \mathbf{B}.\mathbf{y} + \mathbf{C}.\mathbf{x} = \mathbf{l}_s, \tag{3.1a}$$

$$\mathbf{E}.\mathbf{y} + \mathbf{A}.\mathbf{x} = \mathbf{l}_n, \tag{3.1b}$$

where

$$\mathbf{x} = (\mathbf{v}_n, \mathbf{v}_z)^{\mathrm{T}}, \quad \mathbf{y} = (\mathbf{v}_s, \boldsymbol{\xi})^{\mathrm{T}}, \tag{3.2}$$

$$\mathbf{l}_s = \frac{1}{\rho_0}(\mathbf{w}_s^{*(1)}, \mathbf{p}_s^{*(0)}, \mathbf{0})^{\mathrm{T}}, \quad \mathbf{l}_n = \frac{1}{\rho_0}(\mathbf{w}_n^{*(1)}, \mathbf{p}_n^{*(1)}, \mathbf{0})^{\mathrm{T}}, \tag{3.3}$$

$$\left.\begin{aligned} \mathbf{B} &= \begin{bmatrix} \mathbf{R}^{(1)} + i\omega\mathbf{C}^{(1)} & \mathbf{0} \\ \dfrac{\partial \mathbf{C}^{(0)}}{\partial s} & i\omega\mathbf{Z}^{(1)} \end{bmatrix}, \quad \mathbf{D} = \begin{bmatrix} \mathbf{0} & g\hat{\mathbf{C}}^{(0)} \\ \mathbf{C}^{(0)} & \mathbf{0} \end{bmatrix}, \quad \mathbf{E} = \begin{bmatrix} f\mathbf{C}^{(1)} & g\hat{\mathbf{C}}_{\phi n}^{(1)} \\ \mathbf{H}_s^{(0)} & \mathbf{0} \end{bmatrix}, \\ \mathbf{C} &= \begin{bmatrix} f\mathbf{C}^{(1)} & \mathbf{0} \\ \mathbf{C}_{\psi n}^{(1)} & \mathbf{C}_{\psi z}^{(1)} \end{bmatrix} = \begin{bmatrix} \mathbf{C}_1 & \mathbf{0} \\ \mathbf{C}_{\psi n}^{(1)} & \mathbf{C}_{\psi z}^{(1)} \end{bmatrix}, \quad \mathbf{A} = \begin{bmatrix} \mathbf{R}^{(1)} + i\omega\mathbf{C}^{(1)} & \mathbf{0} \\ \mathbf{H}_n^{(1)} & -\mathbf{H}^{(1)} \end{bmatrix} = \begin{bmatrix} \mathbf{A}_1 & \mathbf{0} \\ \mathbf{H}_n^{(1)} & -\mathbf{H}^{(1)} \end{bmatrix} \end{aligned}\right\} \tag{3.4}$$

are complex-valued vectors and matrices. Equations (3.1a, b) consist of two subsystems, a first-order differential equation for the vector quantity $\mathbf{y} = (\mathbf{v}_s, \boldsymbol{\xi})$ and an

algebraic system. The matrices $\mathbf{A}, \ldots, \mathbf{E}$ are expressible in terms of the coefficient matrices of the original system (2.1) and the vectors on the right-hand sides of (3.1 *a*, *b*) are known for prescribed harmonically exciting external forces. Clearly, for an Nth-order model the vectors $\mathbf{x}$ and $\mathbf{y}$ have $2N$ complex-valued components, and so $\mathbf{A}, \ldots, \mathbf{E}$ have the dimension $2N \times 2N$.

The physically relevant boundary condition is no flux through the channel ends, expressible in terms of the variable $\mathbf{y}$ as

$$(\mathbf{I}, \mathbf{0})\,\mathbf{y} = \mathbf{H}\mathbf{y} = \mathbf{0} \quad \text{at} \quad s = 0, L, \tag{3.5a}$$

in which $\mathbf{I}$ is the unit square matrix and $s = 0, L$ mark the channel ends. The two-point boundary-value problem for the ordinary differential equation is given by (3.1) and (3.5*a*), whose numerical solution will now be described.

The preceding equations hold for arbitrary shape functions, but for barotropic motion it suffices to assume $\boldsymbol{\phi} = \boldsymbol{\phi}(n)$. Hence, ${}_1\mathbf{C}_{\phi s} = \mathbf{0}$. The kinematic boundary condition at the bottom, (2.1 *d*), is then separated from the remaining equations, and transforms into a prediction equation for the vertical velocity components, once the horizontal components are known. Setting the v_s determination aside (3.1 *b*) becomes

$$[f\mathbf{C}^{(1)} g\mathbf{C}^{(1)}_{\phi n}]\,\mathbf{y} + [\mathbf{A}_1]\,\mathbf{v}_n = \frac{1}{\rho_0}(\mathbf{w}^{*(1)}_n - \mathbf{p}^{*(1)}_n), \tag{3.5b}$$

and the last term on the left-hand side of (3.1 *a*) reduces to $\mathbf{C}_1\mathbf{v}_n$. Since, moreover, $\mathbf{A}$ and $\mathbf{D}$ are non-singular for non-vanishing cross-sections, the boundary-value problem (3.1)–(3.4) may be written in standard form as

$$\mathbf{y}'(s) = \mathbf{F}(s, \omega)\,\mathbf{y}(s) + \mathbf{g}(s, \omega), \tag{3.6a}$$

$$\left.\begin{aligned} \mathbf{H}\mathbf{y}(0) &= \mathbf{0}, \\ \mathbf{H}\mathbf{y}(L) &= \mathbf{0}, \end{aligned}\right\} \quad \text{with} \quad \mathbf{H} = (\mathbf{I}, \mathbf{0}), \tag{3.6b}$$

where

$$\left.\begin{aligned} \mathbf{F}(s, \omega) &= -\mathbf{D}(s)^{-1}[\mathbf{B}(s, \omega) - \mathbf{C}_1(s)\,(\mathbf{A}_1(s, \omega))^{-1}\,\mathbf{E}(s)], \\ \mathbf{g}(s, \omega) &= \mathbf{D}(s)^{-1}[\mathbf{l}_s - \mathbf{C}(s)\,\mathbf{A}_1(s, \omega)^{-1}\mathbf{l}_n]. \end{aligned}\right\} \tag{3.7}$$

Actually, since (3.6) is complex-valued, and because the matrices $\mathbf{A}, \ldots, \mathbf{E}$ have only a limited number of elements with real and imaginary parts, it is computationally advantageous not to work with (3.6), but with its associated system in which real and imaginary parts are separate. This was done when performing actual calculations, but will not be shown here because one simply obtains another system of the form (3.6) with $4N$ real variables instead of $2N$ complex-valued unknowns. It should also be noticed that (3.6) is written as an inhomogeneous problem. It was solved primarily with the aim of resolving the free-surface oscillation problem. For this, $\mathbf{g} = \mathbf{0}$; the problem then consists of solving for the eigenvalues and associated eigenfunctions. From a practical point of view only the lowest eigenvalues and eigenfunctions are of interest, since they are the most likely to be excited; we shall focus attention on these below.

3.1. *Integration procedure*

There are several methods, all having their particular advantages, for solving the eigenvalue problem associated with (3.6) (see Gary & Helgason 1970). The shooting method may be applied to the linear boundary-value problem (3.6) by superposition of

independent solutions which satisfy the boundary conditions $\mathbf{H}\mathbf{y}(0) = \mathbf{0}$ at $s = 0$. In this case the solution may be expressed as

$$\mathbf{y}(s) = \sum_{i=1}^{N} \mathbf{u}_i(s)\, c_i + \mathbf{w}(s), \tag{3.8}$$

where the vectors $\mathbf{u}_i(s)$ of dimension $2N$ are linearly independent solutions of the homogeneous system (3.6):

$$\mathbf{u}_i' = \mathbf{F}(s, \omega)\, \mathbf{u}_i(s). \tag{3.9}$$

The solutions are computed by integrating (3.6*a*) as an initial-value problem subject to the homogeneous initial conditions (3.6*b*) at $s = 0$. The vector $\mathbf{w}$ is a particular solution of (3.6*a*) also subject to the boundary condition at $s = 0$. The c_i are constants of superposition, and may be determined from the second boundary condition

$$\mathbf{H}\mathbf{y}(L) = \mathbf{H}(\mathbf{U}(L)\,\mathbf{c} + \mathbf{w}(L)) = \mathbf{H}\mathbf{U}(L)\,\mathbf{c} + \mathbf{H}\mathbf{w}(L) = \mathbf{0}, \tag{3.10}$$

where $\mathbf{U}$ is the matrix with column vectors $\mathbf{u}_i$, and $\mathbf{c}$ is the vector of the free constants c_i. If the matrix $\mathbf{H}\mathbf{U}(L)$ is non-singular, the unknown vector $\mathbf{c}$ may be determined from (3.10) and the solution may be computed from (3.8).

Formally, for the case of free oscillations the inhomogeneous solution is $\mathbf{w} \equiv \mathbf{0}$; (3.10) has only non-trivial solutions provided that $\mathbf{H}\mathbf{U}$ is singular. For a lake with length L this will yield a discrete frequency spectrum and associated eigenfunctions. The latter are obtained by calculating $\mathbf{c}$ (up to a free amplitude) and resubstituting it into (3.8).

The above procedure to determine the complementary functions $\mathbf{u}_i$ ($i = 1, \ldots, N$) and to evaluate the eigenfrequency from a singularity condition of the system $\mathbf{H}\mathbf{U}(L, \omega)\,\mathbf{c} = \mathbf{0}$ would work perfectly, were it not for the numerical properties of the matrix $\mathbf{F}$ (in (3.6)). Numerical calculations for realistic values of ω show that the spectral width of the matrix $\mathbf{F}$ is generally large, and furthermore increases with increasing number of shape functions. As a result complementary functions lie far apart; although they are theoretically linearly independent they are numerically (nearly) linearly dependent, making the system (3.10) computationally ill-conditioned.

This situation is nevertheless well known to numerical analysts. A way of overcoming the difficulties is to divide the interval $[0, L]$ into subintervals that are sufficiently small so that the complementary solutions within each subinterval cannot lie too far apart at the end of the subinterval; at the end of each subinterval the complementary vector $\mathbf{c}$ is transformed by a Gram–Schmidt orthonormalization procedure, and integration is continued with this new orthonormalized initial vector. This process is continued until the other end $s = L$ is reached, where the second boundary condition is satisfied.

The integration procedure described above is known in numerical analysis as the *initial-value approach coupled with orthonormalization*, and excellent software packages exist, with the aid of which the integration can be implemented (see e.g. Scott & Watts 1975; Watts, Scott & Lord 1979); for a detailed description of the numerical treatment of the channel equations, see Raggio (1981). In our analysis the SUPORT package of Scott *et al.* was used, and results discussed below pertain to its use in our lake model.

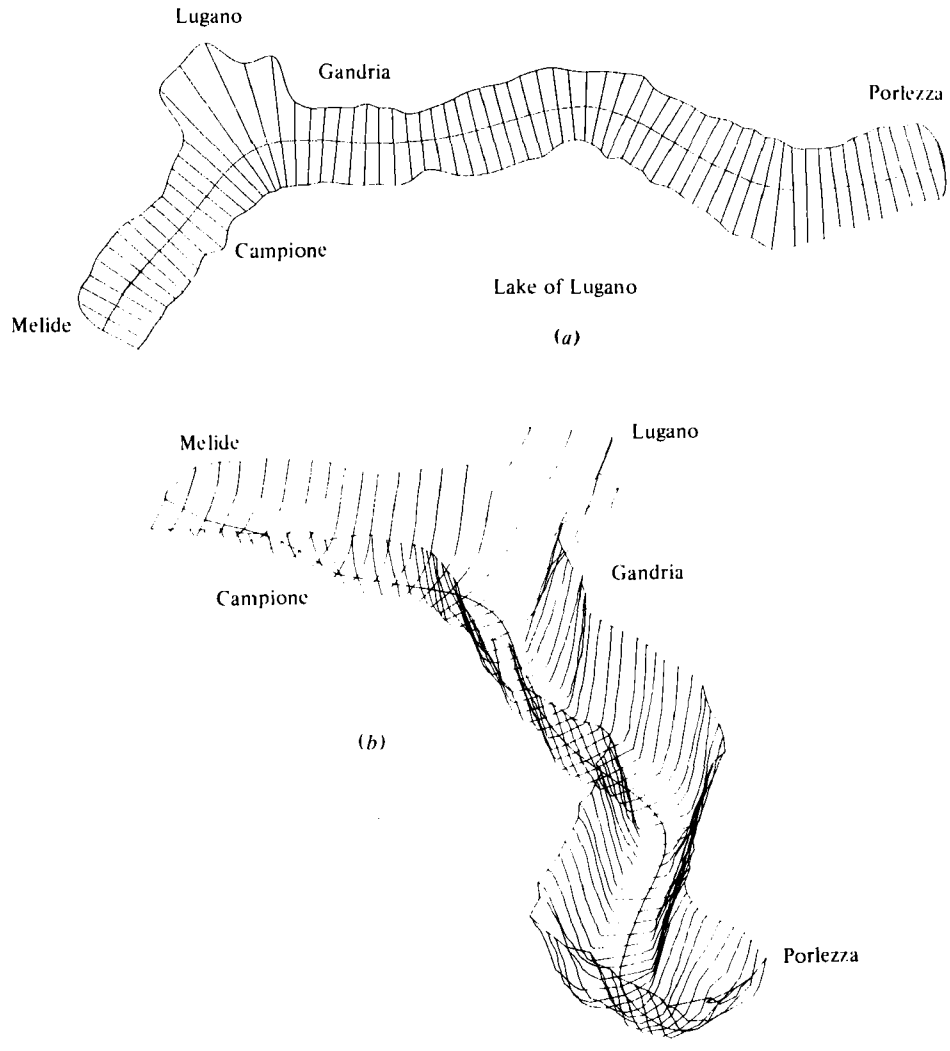

FIGURE 1. (*a*) Top view of the channel-model discretization: cross-sections and axis. (*b*) Perspective view of the channel-model discretization: cross-sections and thalweg.

3.2. *The seiches of the Eastern basin of Lake of Lugano*

The Eastern basin of the Lake of Lugano is a very narrow, extremely deep, L-shaped channel with a length of about 17 kilometers. The mean lake width is 1·5 km, with a minimum width of 1 km and a maximum width of 3 km. The Lake has steep shores, and the mean depth is 175 m, with a maximum depth of 287 m. The ends of this channel-like lake are shallow compared with the remainder of the basin. Figure 1 (*a*) shows a top view of the Lake, including the selected axis and cross-sections. In figure 1 (*b*) a perspective view of the channel-model discretization is shown. Cross-sections and thalweg are plotted.

Numerical results should depend on the choice of shape function, but careful study (Raggio 1981, 1982) has indicated that for polynomial shape functions surface elevation plots do not depend appreciably on this selection. The following results are based on

Mode	Finite-element model		Channel model	
	Frequency ($\times 10^{-1}$ Hz)	Period (min)	Frequency ($\times 10^{-1}$ Hz)	Period (min)
1	0·075	13·8	0·076	13·7
2	0·158	6·6	0·161	6·5
3	0·206	5·1	0·210	5·0
4	0·278	3·8	0·280	3·7

TABLE 1. Eigenfrequencies of the four lowest gravitational surface seiches for the eastern basin of the Lake of Lugano as obtained with Hamblin's finite-element model and the channel model with 4 Cauchy terms as shape functions

a four-term Cauchy-series expansion $\boldsymbol{\phi} = \{1, n, n^2, n^3\}$, but later on suitably selected orthogonal polynomials will be used. These are chosen so as to make $\mathbf{C}^{(1)}$ diagonal. Results were constructed for the first four modes, and these were compared with those obtained from a finite-element representation of the tidal equations. This finite-element program is due to Hamblin (personal communication).

The eigenfrequencies of the four lowest-order surface gravitational modes are shown in table 1. The two methods yield practically the same eigenfrequencies, as the difference in all calculated periods is only about 6 s. This difference is associated mainly with the form in which the lake was discretized in the two models.

A verification of the surface seiches with actual data was possible, as water-level measurements around the Lake of Lugano were gauged with instruments from the Swiss Hydrological Survey (Bern). The gauges restricted the frequency range in which seiches are found to the lowest three modes, and did not allow detection of phase shifts by which the rotation of amphidromies could have been verified. Smoothed power spectra of surface-elevation gauges positioned at Campione, Lugano and Porlezza, however, allowed identification of the frequencies of the first three modes. Time series are from an event that took place in the late afternoon of 9 August 1979, when violent wind gusts from a Western direction strongly excited the free oscillation modes of the lake.

Figure 2 shows the smoothed power spectra for these stations for the time series of the surface elevation gauges between 7.55 p.m. and 3.15 a.m. on 9 and 10 August 1979. The first three eigenfrequencies as calculated with the channel model are indicated with arrows. The first calculated eigenfrequency is obviously excited at the three stations, and for frequencies corresponding to the second and third calculated modes corresponding peaks in the power spectra may be identified. The differences between the peaks in the data and the predicted frequencies may be attributed to imprecision in the recording of these high frequency oscillations, since the errors are not systematic. Other relative maxima can also be identified which are not predicted by the model. These cannot be attributed to an interaction between the Western and Eastern basin of the Lake of Lugano. Such an interaction behaves like a Helmholtz resonator (Neumann 1944) which has a frequency far below the first eigenfrequencies of the single basins. They cannot be attributed to nonlinear effects, since the amplitudes are very small. The only apparent reason is that the atmospheric forcing had these dominant frequencies.

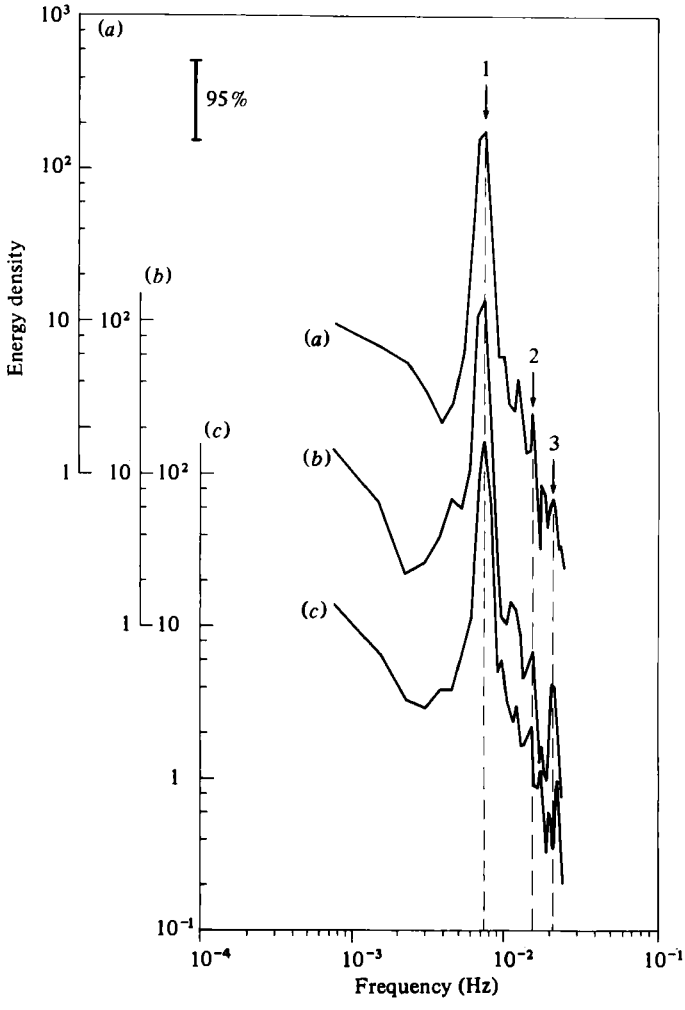

FIGURE 2. Power spectra of the surface-elevation oscillation for the stations Campione (*a*), Lugano (*b*) and Porlezza (*c*). Energy density = $0{\cdot}36 \times 10^{\text{ordinate}}$ in m^2/s. The arrows marked by 1, 2, and 3 indicate the first three eigenfrequencies of the lake.

Figures 3(*a–d*) display for the channel model the co-range and co-tidal lines of the four lowest eigenmodes of the basin. When $\xi = \xi_0 \exp(i(\omega t - \beta))$ the former are the lines of constant real ξ_0 and the latter those of constant β. The normalization for both is arbitrary; ξ is normalized so as to give the maximum amplitude the value 100 units. The equidistance of the co-range lines is equal to 10 units, and the co-tidal lines are represented for the values $\beta = 0°$, $0{\cdot}1°$, $179{\cdot}9°$, $180°$, $180{\cdot}1°$ and $359{\cdot}9°$. Co-range and co-tidal lines were plotted with a contour-plot program for orthogonal curvilinear co-ordinates. Inspection of the co-tidal lines indicates that all amphidromies rotate in the counter-clockwise direction. The motion in the lake is consequently of Kelvin type.

The lowest mode has a single ampidromic point roughly at the middle of the lake. Co-tidal lines are strongly bundled in the cross-channel direction. The longitudinal

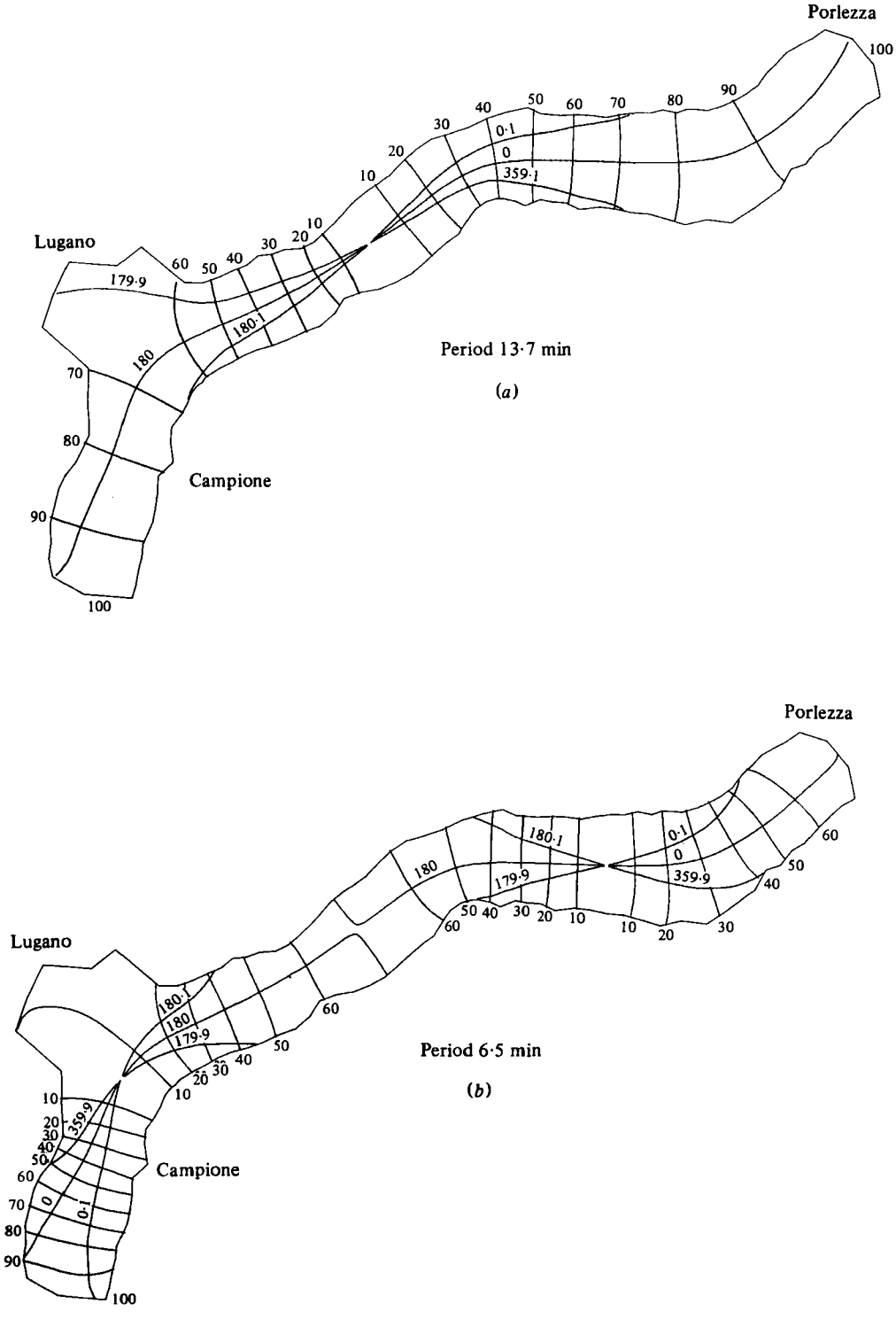

FIGURE 3(*a*, *b*). For caption see p. 292.

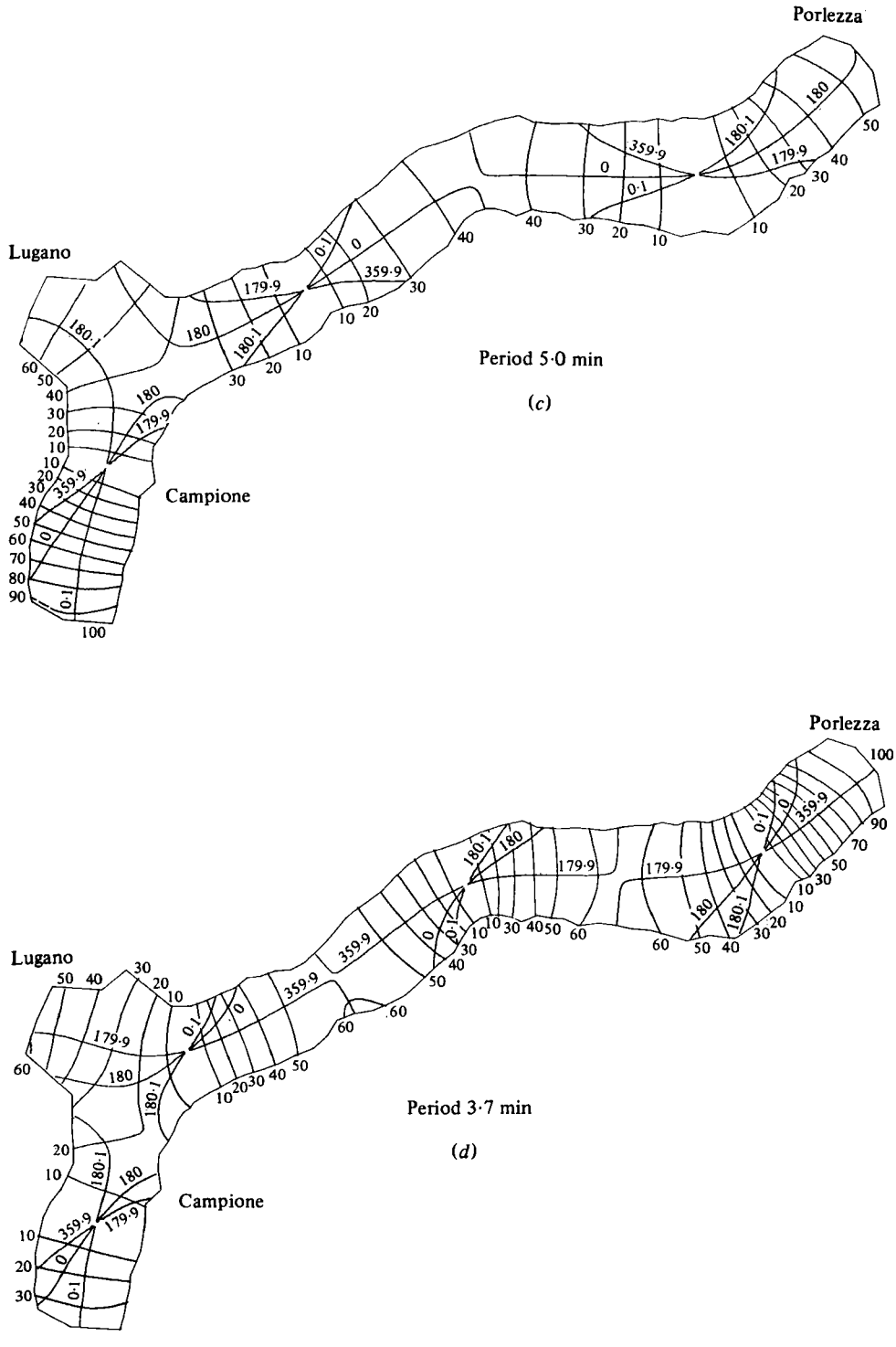

FIGURE 3. Channel model: amphidromic systems for the first (*a*), second (*b*), third (*c*) and fourth (*d*) gravitational modes. Cauchy series; 4 shape functions.

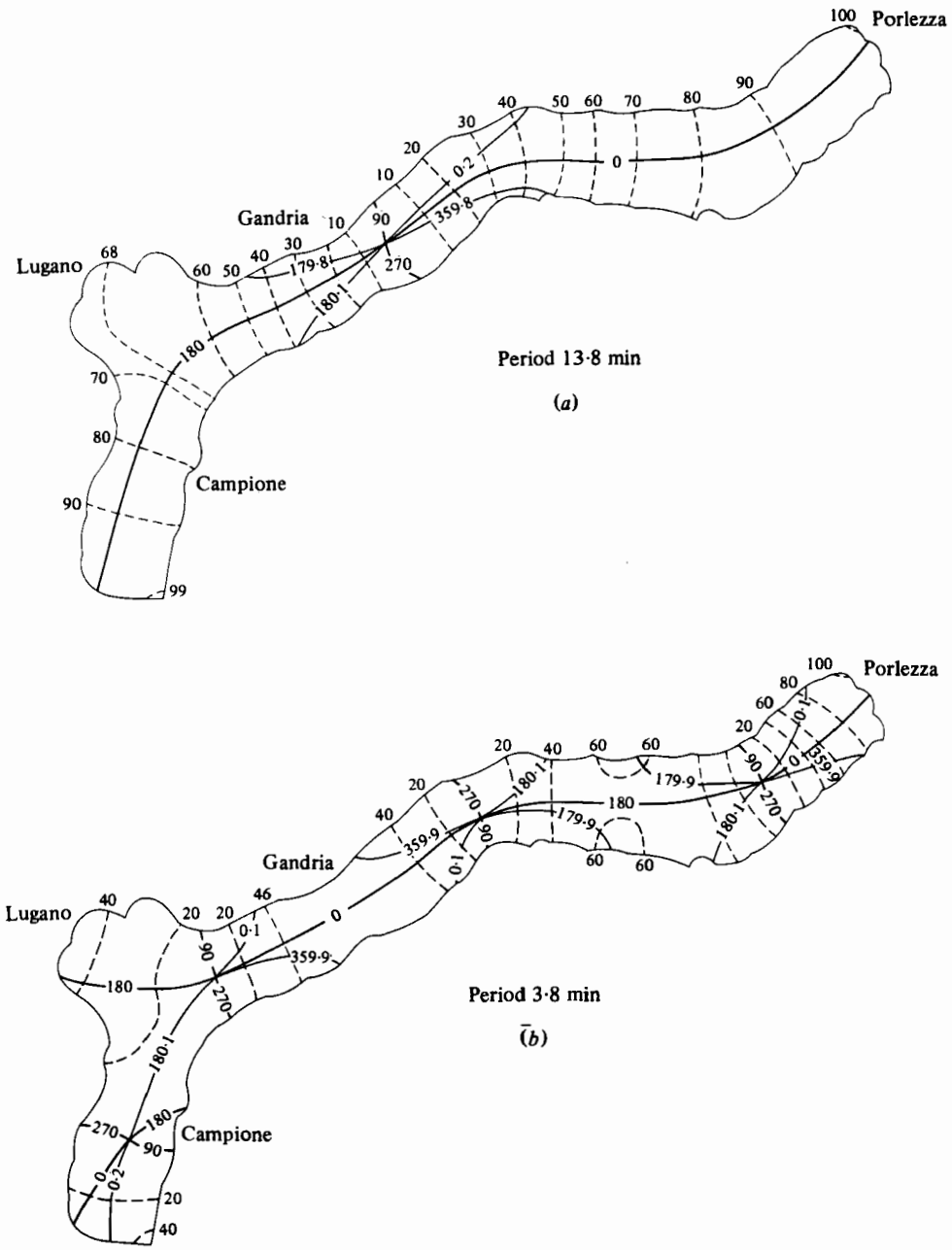

FIGURE 4. Finite-element model: amphidromic systems for the first (*a*) and fourth (*b*) gravitational modes.

structure of the oscillation is manifested by this bundling, and because co-range lines all join points of opposite shores. This behaviour persists even in the vicinity of the Bay of Lugano (the shallow wide portion of the lake close to Lugano). The preference for longitudinal behaviour persists for the second mode, even though an amphidromic point is situated near the Bay of Lugano. The third and fourth mode exhibit still mainly

Number of shape functions	Mode 1×10^{-2} Hz		Mode 2×10^{-1} Hz	
	Frequency	Differences	Frequency	Differences
1	0·768063		0·287213	
		0·0016		0
2	0·766446		0·287213	
		0·0018		0·0063
3	0·764672		0·280926	
		0·0004		0·0009
4	0·764257		0·280017	
Extrapolated	0·762877		0·277845	

TABLE 2. Eigenfrequencies for the eastern basin of the Lake of Lugano for the first and fourth gravitational modes using one, two, three and four Cauchy terms as shape functions and an extrapolated value

longitudinal behaviour, but in the Bay of Lugano surface elevations now show a strong gradient transverse to the main channel direction, as there are now co-range lines connecting points on the same shoreline.

A more challenging test of the suitability of the channel model than a frequency comparison is obtained by comparing the eigenmode structures with those based on Hamblin's finite-element model. Figures 4 (a, b) show the corresponding amphidromic systems for mode 1 and mode 4, based on the finite-element representation using triangular elements with quadratic shape functions. Bearing in mind that contour plots for the channel model were produced with a contour-plot program while those for the finite-element calculations were drawn by hand, agreement must be regarded as excellent. It should further be noticed that the finite-element grid used was too coarse for the spatial resolution of the fifth and higher modes; in contrast, the fifth mode was reproduced without any difficulties with the channel model.

Further tests regarding the accuracy of the model were undertaken, among these, differences in results were analysed when varying the number of terms considered in the Cauchy-series expansion. Calculations show broadly that, for each mode, increasing the number of shape functions incorporated in the model will decrease the difference in subsequent eigenfrequencies, presumably to an asymptotic value. The eigenfrequencies obtained with one to four shape functions, the difference between them, and extrapolated values for each mode are listed in table 2. It is evident that the one-term model allows determination of the eigenfrequencies with sufficient accuracy for surface seiches. Structurally, the one-term model, corresponding to the Chrystal model, shows purely longitudinal standing waves with four nodal lines. The two-term model exhibits the onset of transverse oscillation in the vicinity and within the Bay of Lugano. This behaviour becomes more pronounced with increasing number of shape functions. Nonetheless the results suggest that from the structure of the eigenmodes of such an elongated lake it appears to be sufficient to work with a two-term model to describe surface seiches properly.

4. Further discussions and concluding remarks

The results obtained in I and II and in the above prove the suitability of the model equations as far as free gravitational oscillations are concerned. An analysis of forced oscillations described below turned out to indicate clearly firstly the sensitivity of the results with respect to the shape function choice, and secondly the limitation of the

applicability of the model to gravitational modes. Generally, shape functions may be selected from physically meaningful assumptions of the particular phenomenon one would like to simulate or from considerations regarding a minimization of the computational effort. The latter suggests the use of orthogonal families, generated by inner products of the form

$$(P_i, P_j) = \int_a^b w(n)\, P_i(n)\, P_j(n)\, dn = \begin{cases} \|P_i\| & (i = j), \\ 0 & (i \neq j), \end{cases} \tag{4.1}$$

in which P_i and P_j are two members of the family and w is a weighting function. Orthogonal polynomial families are computationally particularly advantageous, since they can be constructed with three-term recursive formulas.

The idea is to select shape functions ϕ_i that diagonalize a particular submatrix in (3.1) and are thus orthogonal with respect to that inner product. Raggio (1982) shows that the most convenient choice is to make the matrix

$$C_{ij}^{(1)} = (\phi_i, \phi_j) = \int_{B^-}^{B^+} JH(n)\, \phi_i(n)\, \phi_j(n)\, dn, \tag{4.2}$$

diagonal or equal to the unit matrix (see (3.4)). Within the class of polynomial families the ϕ_i must be numerically evaluated. With $\phi_j = \Sigma_{\nu=0}^{3} a_\nu(s)\, n^\nu$ this amounts to the evaluation of the coefficients a_ν along the channel axis.

To illustrate the dependency of the computational results on the choice of shape function, consider the *frequency response* to a harmonic West–East wind with amplitude of 10 m/s. The wind stress w_i is then represented by

$$w_i = \rho_{\text{air}}\, c_{\text{wind}}\, v_{\text{wind}},$$

with $\rho_{\text{air}}\, c_{\text{wind}} = 1{\cdot}2\,\text{kg/m}^2\text{s}$ and $v_{\text{wind}} = 10\,\text{m/s}$. With these, a frequency-domain comparison was made using three terms in the Cauchy series, orthogonal and orthonormal polynomials. The frequency range from 3×10^{-4} Hz to 3×10^{-1} Hz was sampled with a logarithmic increment of 13·5 Hz to show roughly how the lake reacts at the different frequencies. Figures 5(*a*, *b*, *c*) show the surface-elevation response at the stations of Campione, Lugano and Porlezza for the three types of shape function. The frequencies of the first four gravity modes are marked with arrows to show the near-resonance behaviour around these frequencies. The exact behaviour very close to single eigenfrequencies is not shown properly because of the coarse logarithmic frequency increment. It is interesting that the different types of shape function shift the individual eigenfrequencies slightly. That is why, for example, the orthonormal polynomials show strong response at the second eigenfrequency, while the Cauchy series and the orthogonal polynomials do not, since the exact second eigenfrequency has been slightly missed by the sampling in the last two cases. The only fundamental difference in response for the three different shape functions is found around the frequency of 1×10^{-3} Hz where the amplitude of the surface oscillations near Porlezza falls rapidly for Cauchy-series and orthogonal-polynomial shape functions but not for orthonormal polynomials. This warrants further study.

It should also be pointed out that the channel model has been found suitable in the range of gravitational modes where the currents are essentially irrotational and driven by pressure gradients caused by differences in the surface elevation of the lake. Below the inertial frequency the motion is basically non-divergent, rotational and not

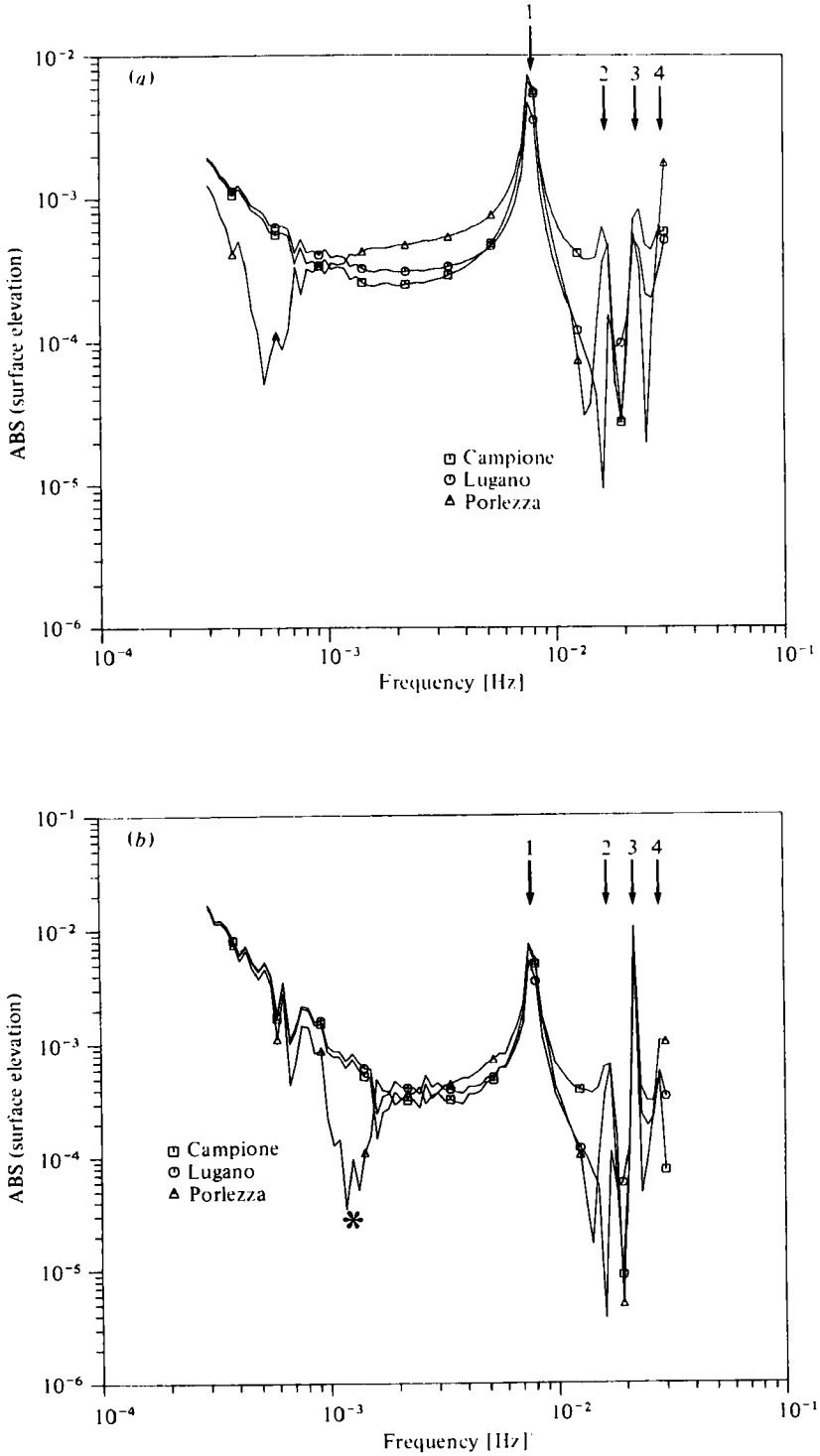

FIGURE 5(*a*, *b*). For caption see facing page.

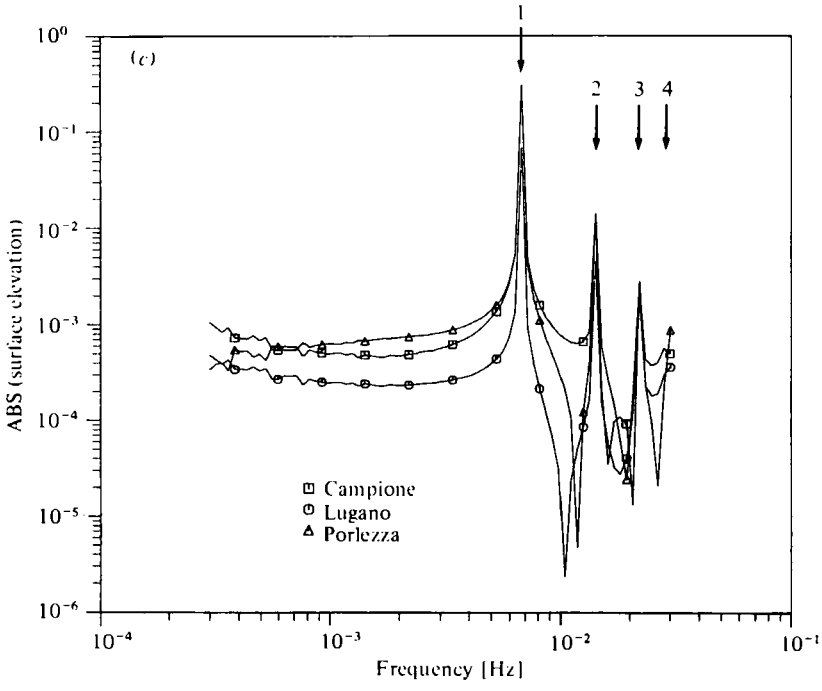

FIGURE 5. Response of the surface elevation amplitude in metres at the stations of Campione, Lugano and Porlezza, using as shape functions three terms of (*a*) a Cauchy series, (*b*) orthogonal polynomials, and (*c*) orthonormal polynomials.

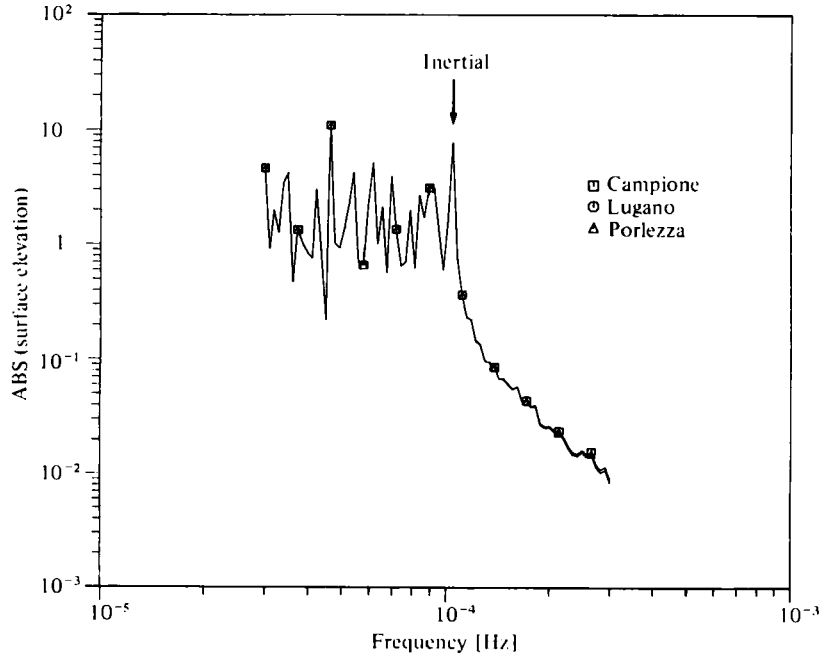

FIGURE 6. Response of the surface-elevation amplitude in metres at the stations of Campione, Lugano and Porlezza for a frequency range near the inertial frequency. Three terms of orthogonal polynomials are used as shape functions. (All three symbols for the positions Campione, Lugano and Porlezza are so close that on the scale of this plot a single curve is seen.)

primarily dependent on the surface-elevation distribution but rather on depth variation. This is the domain of *topographic waves* for which we have encountered difficulties which are not yet resolved. The difficulties with the present approach are perhaps best seen when the frequency response to the harmonic East–West wind is pursued to subinertial frequencies. Figure 6 displays the absolute value of the surface elevation at the Campione, Lugano and Porlezza stations for frequencies near the inertial frequency. It is clear from this figure that with our approach the mentioned subinertial frequencies cannot be properly predicted. The reason is that the channel equations contain surface-wave information which must be filtered out to enable the numerical procedure to identify the essential character of the motion in that range. This suggests the use of a rigid lid. On the other hand it was seen in II when discussing wave reflection in rectangular canals that the differential equations of the channel model must become *stiff* at very small frequencies. This would suggest the use of numerical integrators for stiff equations. The entire problem is not clear at the moment and warrants further study.

While performing this work G. Raggio was financially supported by the Swiss National Science Foundation through the national programme 'Basic Problems of the Swiss Water Budget', Contract no. 4.006.0.76.02. We are grateful to Dr P. Hamblin for his permission to use his program and to report results obtained with it.

REFERENCES

GARY, J. & HELGASON, R. 1970 A matrix method for ordinary differential equation eigenvalue problems. *J. Comp. Phys.* **5**, 169–187.

HAMBLIN, P. F. 1972 Some free oscillations of a rotating natural basin. Ph.D. thesis, Univ. of Washington, Seattle.

HAMBLIN, P. F. 1976 Seiches, circulation and storm surges of an ice-free Lake Winnipeg. *J. Fish. Res. Board* **33**, 2377–2391.

NEUMANN, G. 1944 Die Impedanz mechanischer Schwingungssysteme und ihre Anwendung auf die Theorie der Seiches. *Ann. Hydr. Mar. Met.* **72**, 65–79.

RAO, D. B. 1966 Free gravitational oscillations in rotating rectangular basins. *J. Fluid Mech.* **25**, 523–555.

RAO, D. B. 1973 Spectral methods of forecasting storm surges. *Hydrological Sci. Bull.* **18**, 311–316.

RAO, D. B. 1977 Free internal oscillations in a narrow rotating rectangular basin. In *Modeling of Transport Mechanisms in Oceans and Lakes* (ed. T. S. Murty), pp. 391–398.

RAO, D. B. & SCHWAB, D. J. 1976 Two dimensional normal modes in arbitrary enclosed basins on a rotating Earth: application to Lakes Ontario and Superior. *Phil. Trans. R. Soc. Lond.* A **281**, 63–96.

RAGGIO, G. 1981 A channel model for a curved elongated homogeneous lake. Dissertation, Eidgenössische Technische Hochschule Zürich. *Mitteilung* Nr 48 *der Versuchsanstalt für Wasserbau, Hydrologie und Glaziologie, ETH Zürich.*

RAGGIO, G. 1982 On the Kantorovich technique applied to the tidal equations in elongated homogeneous lakes. *J. Comp. Phys.* (to appear).

RAGGIO, G. & HUTTER, K. 1982*a* An extended channel model for the prediction of motion in elongated homogeneous lakes. Part 1. Theoretical introduction. *J. Fluid Mech.* **121**, 231–255.

RAGGIO, G. & HUTTER, K. 1982*b* An extended channel model for the prediction of motion in elongated homogeneous lakes. Part 2. First-order model applied to ideal geometry: rectangular basins with flat bottom. *J. Fluid Mech.* **121**, 257–281.

SCHWAB, D. J. 1978 Simulation and forecasting of Lake Erie storm surges. *Mon. Weather Rev.* **106**, 1477–1487.

SCOTT, M. R. & WATTS, H. A. 1975 A computer code for two-point boundary value problem via orthogonalization. *Sandia Labs, Albuquerque* SANDIA-75-0198.

WATTS, H. A., SCOTT, M. R. & LORD, M. E. 1979 Solving complex valued differential systems. *Sandia Labs, Alburquerque* SANDIA-78-1501.